Flexural crack control in fiber-reinforced concrete according to AS3600

Received: 10 February 2025 | Revised: 25 June 2025 | Accepted: 13 July 2025

DOI: 10.1002/suco.70255

ARTICLE

fib CEB-FIP WILEY

Flexural crack control in fiber-reinforced concrete according to AS3600

Ali Amin[1] | **R. Ian Gilbert**[2] | **E. Stefan Bernard**[3]

[1]School of Civil Engineering, The University of Sydney, Sydney, New South Wales, Australia

[2]School of Civil and Environmental Engineering, The University of New South Wales, Sydney, New South Wales, Australia

[3]Institute for Sustainable Industries and Liveable Cities (ISILC), Victoria University, Melbourne, Victoria, Australia

Correspondence
Ali Amin, School of Civil Engineering, The University of Sydney, Sydney, New South Wales, Australia.
Email: ali.amin@sydney.edu.au

Funding information
Australian Research Council, Grant/Award Numbers: DP200102114, IE240100025

Abstract

This paper provides an overview and background for the expressions given in the draft Australian Concrete Structures Standard (AS3600-202X) with respect to flexural crack widths in fiber-reinforced concrete (FRC) elements containing conventional reinforcement. The proposed model has been adapted from the existing expression for plain reinforced concrete and accounts for the beneficial effects of the fibers (steel and polypropylene) in the short- and long-term and accounts for behavior observed in large-scale long-term test data. The benefit of this approach is that a single (unified) expression may be used to determine the short- and long-term cracking behavior of conventionally reinforced or FRC elements subjected to flexure.

KEYWORDS

cracking, fiber-reinforced concrete, flexure, serviceability, shrinkage

1 | INTRODUCTION

Serviceability limit state design has increasingly played a more prominent role in the design of reinforced concrete beams and slabs in recent years. Although cracks are common in structural concrete, excessive or uncontrolled cracking can significantly influence the serviceability and durability of structural concrete. This is in addition to any esthetic requirements that a structural element may have. The control of cracking in structural concrete has traditionally been achieved by limiting the stress in the conventional reinforcement traversing a crack to an appropriately low value (which is typically specified in codes of practice) and ensuring that the reinforcement is suitably distributed within the tensile zones of the element. The drawback of such an approach is that, typically, large amounts of reinforcement are required to limit crack widths, and hence the economic consequences are significant.

The control of cracking in structural concrete elements containing steel or macro-synthetic fiber reinforcement is well documented in the literature.[1–4] Conventionally reinforced concrete members that also contain fibers (commonly referred to as fiber-reinforced concrete [FRC]) generally present finer and more closely spaced cracks than the same member not containing fibers—assuming both members contain equal amounts of conventional reinforcement. The foremost advantage of introducing fibers to structural concrete is their ability to transmit tension across cracks. This phenomenon has been well documented for elements failing in shear.[5,6] In a serviceability analysis, when both fibers and conventional steel reinforcements traverse a crack, the stress across the crack is shared between these two contributors.[7] For example,

consider the two long tension chords with un-yielded reinforcement subjected to uniaxial tension presented in Figure 1. The tension chord illustrated in Figure 1a contains fibers, whereas the tension chord in Figure 1b does not. For a given load P (which is greater than the load required to induce cracking), the fibers at the crack are engaged and transmit a tensile stress equivalent to $\sigma_f(w)$ across the crack. $\sigma_f(w)$ is primarily dependent on the type and volume of fibers but is also indirectly affected by factors such as the compressive strength of the concrete. For the tension chord not containing fibers, the tension at the crack is taken wholly by the reinforcing steel. The proportion of stress carried by the conventional steel and the fibers is primarily dependent on the quantity of each reinforcement. The contribution of the fibers to the overall tension across a crack decreases significantly as the crack widens. This is due to the strain-softening nature of most fiber types and dosages used in practice. Widening of cracks can be attributed to an increase in applied load and/or to shrinkage of the concrete between the cracks. According to the Tension Chord Model for FRC (see Refs. 8,9) (and for reinforced concrete see Ref. 10), there is a build-up of tension in the uncracked concrete with distance from each crack (the magnitude of which is a function of the bond between the reinforcement and surrounding concrete, the reinforcement ratio, and the diameter of the reinforcement) and this tensile stress is limited to the tensile strength of the concrete, f_{ct}, with a maximum value located mid-way between the cracks. Consequently, it can be demonstrated that the crack spacing in FRC elements can be significantly reduced by increasing the fiber content or post-cracking performance—this has significant implications for predictions of crack widths in FRC members.

The authors have previously developed and verified models for the prediction of cracking and deformation of FRC flexural elements using the Tension Chord Model (shown in Figure 1 and described above)—see Amin et al.[11] and Markic et al.[12] Some of these models require an iterative solution and are not unified with the crack control expressions contained in Australian Concrete Structures Standard (AS3600-2018[13]) for reinforced concrete. It should be noted that the existing provisions contained within AS3600-2018 for determining the cracking behavior of FRC flexural elements containing conventional reinforcement do not adequately account for physical observations made in large scale, long-term testing. To this end, existing expressions contained for determining the short- and long-term flexural crack widths of reinforced concrete are extended to FRC members in a manner that is consistent with experimental observations.

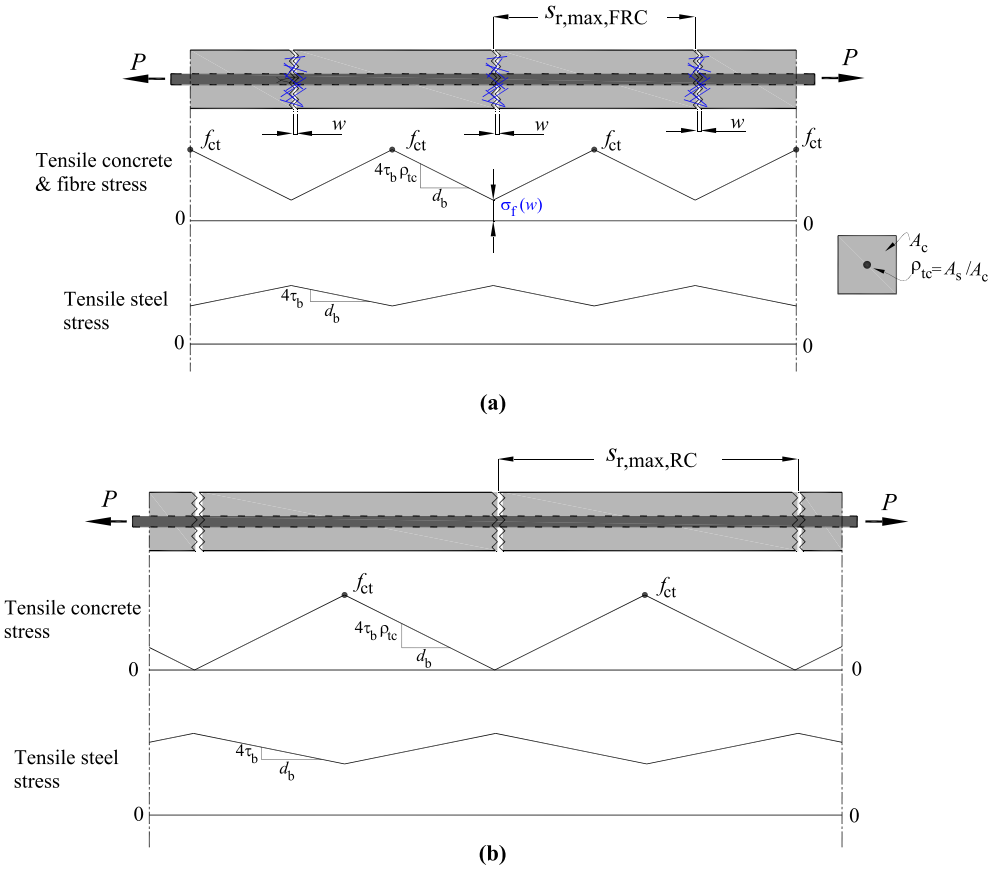

FIGURE 1 Cracking behavior of tension chords: (a) fiber-reinforced concrete (FRC); (b) RC.

2 | SIMPLIFIED CODE APPROACHES FOR FLEXURAL CRACK CONTROL

Several codes of practice contain provisions to evaluate flexural crack widths in reinforced concrete structures (*fib* MC2010,[14] *fib* MC2020,[15] Eurocode 2,[16,17] and AS3600[13]). These models predict crack widths at any time after cracking based on the integral of the difference between the mean strain in the steel reinforcement and the mean strain in the concrete between two cracks:

$$w = s_{r,max}(\varepsilon_{sm} - \varepsilon_{cm}). \quad (1)$$

In Equation (1), w is the maximum design crack width (as opposed to the absolute maximum crack width), $s_{r,max}$ is the maximum crack spacing, ε_{sm} is the mean strain in the steel reinforcement between the cracks at the serviceability design load, and ε_{cm} is the mean strain in the concrete between the cracks. Available models apply various simplifications to determine the crack spacing and strain difference (see Refs. 18–21). The application of Equation (1) depends on the model used to describe the transfer of load between the reinforcement and the surrounding concrete through mechanical interlock. The "no-slip" approach assumes that perfect bond exists between the steel reinforcement and the surrounding concrete. This approach has been used in nonlinear finite element analyses combined with concrete damage plasticity models to adequately predict the cracking behavior of reinforced concrete elements.[22] More common, however, is the "slipping-bond" approach. In this method, slip (i.e., relative displacement) is assumed to occur between the steel reinforcement and the concrete. The slip can be evaluated by solving a second-order differential equation for a given bond stress–slip relationship. In this approach, the slip is a maximum at the crack and diminishes to zero moving away from the crack.

2.1 | Crack spacing

Various expressions have been developed for the determination of crack spacings in conventionally reinforced and FRC elements subjected to flexure (see Refs. 8,23–25; Amin and Gilbert [4]). It is important to note that maximum crack spacings are of interest (as opposed to average crack spacings) when seeking to estimate design crack widths. Referring back to the tension chords shown in Figure 1, where it is assumed that the development of stress within the FRC between the cracks is the same for concrete with and without fibers, and is a function of the bond between the reinforcing steel and concrete matrix, τ_b, the reinforcement ratio ($\rho_{tc} = A_{st}/A_{ct}$) and the diameter of the steel reinforcement, d_b, assuming constant bond stresses τ_b. The stress ($\sigma_{tc}(x)$) within the tensile concrete at any point x along the tension chord between a primary crack ($x = 0$) and the location between any two primary cracks ($x = s_{r,max}/2$) is equal to:

$$\sigma_{tc}(x) = \sigma_f(w) + \frac{4\tau_b\rho_{tc}x}{d_b} \ldots 0 \le x \le \frac{s_{r,max}}{2}. \quad (2)$$

Setting Equation (2) to f_{ct} at $x = s_{r,max}/2$ yields an expression for $s_{r,max}$:

$$s_{r,max} = \frac{d_b(f_{ct} - \sigma_f(w))}{2\tau_b\rho_{tc}} \ge l_f. \quad (3)$$

The limiting term in Equation (3), l_f, is the fiber length and was introduced by Kaufmann et al.[26] For large fiber dosages (i.e., for $\sigma_f(w) \sim f_{ct}$), Equation (3) may yield very small crack spacings. This is, however, physically impossible, as for small crack openings, the embedment length of the fibers would be too short to develop enough tension to warrant such stresses. Substituting $\sigma_f(w) = f_{0.5}$ (i.e., the residual tension offered by the FRC at a crack opening displacement equal to 0.50 mm) in Equation (3) has been shown to provide reasonable results. It is noted that setting $\sigma_f(w)$ equal to zero gives the same relationship as in the original Tension Chord Model by Marti et al.[10]

In the Tension Chord Model approach described above, the tensile concrete stresses are assumed to be uniformly distributed over the tension chord, implying plane concrete sections and leading to equal crack widths from the bar to the concrete surface. It is important to recognize that crack widths at the concrete surface will differ from crack widths if they are measured at the steel–concrete interface, as explained in Beeby.[27] Furthermore, experiments on reinforced concrete elements in flexure have demonstrated that concrete cover, c, the distribution of reinforcement in the tensile zone, and the longitudinal strain distribution each have a considerable influence on the maximum crack spacing.[23] Consequently, AS3600-2018 has adapted the 2004 version of Eurocode 2 for determining maximum crack spacings in reinforced concrete elements. This method originated in 1966 when Ferry-Borges[28] combined the contributions of concrete cover and slipping bond. For cross-sections with bonded reinforcement fixed at reasonably close centers (i.e., at bar spacings less than $5(c + 0.5d_b)$), the maximum crack spacing is determined as:

$$s_{r,max} = k_{f2}\left(3.4c + \frac{0.3k_1k_2d_b}{\rho_{eff}}\right) \le 1.3(D - d_n). \quad (4)$$

In Equation (4), ρ_{eff} is the reinforcement ratio given by $A_{st}/A_{c.eff}$ where $A_{c.eff}$ is the effective area of concrete

in tension surrounding the bars with depth $h_{c.eff}$ equal to the lesser of 2.5 $(D - d)$, $(D - d_n)/3$ or $D/2$ where d is the effective depth of the section, D is the total depth of the section and d_n is the depth to the neutral axis. k_1 is a coefficient that accounts for the bond properties of the bonded reinforcement, $k_1 = 0.8$ for deformed bars and 1.6 for plain bars; k_2 is a coefficient that accounts for the longitudinal strain distribution through the depth of the section with $k_2 = 0.5$ for pure bending and $k_2 = 1$ for pure tension. For cases in combined tension and bending, $k_2 = (\varepsilon_1 + \varepsilon_2)/(2\varepsilon_1)$ where ε_1 is the greater and ε_2 is the lesser of the tensile strains at the boundaries of the cross-section (assessed on the basis of a cracked section). Caldentey et al.[29] criticized this approach for tension elements, noting that this method leads to very exaggerated crack spacings and also noting that there are fundamental differences in the cracking behavior of reinforced concrete elements subjected to either direct tension or pure bending. The new crack width provisions in Eurocode 2:2024 have been influenced by this rationale. For a description of the cracking behavior of FRC elements subjected to pure tension, we refer to the recent study by Tang et al.[30] Where a mixture of bar diameters is used in a section, an equivalent bar diameter, $d_{b.eq}$, is used. For a section with n_1 bars of diameter d_{b1} and n_2 bars of diameter d_{b2}, the following expression is used:

$$d_{b.eq} = \frac{n_1 d_{b1}^2 + n_2 d_{b2}^2}{n_1 d_{b1} + n_2 d_{b2}}. \tag{5}$$

The term k_{f2} shown in Equation (4) is a modification factor introduced in this study to account for the effect of the fibers (if any) on crack spacing. As can be inferred from Equation (3), in general, the greater the residual strength offered by the fibers, the greater the reduction in crack spacing. For a section not containing fibers, $k_{f2} = 1.0$. For a section containing fibers, k_{f2} is taken as:

$$k_{f2} = 1 - \frac{1.1 k_g k_{f3} f_{0.5}}{f_{ct}}. \tag{6}$$

In Equation (6), k_g is a member size factor equal to $1 + (0.0067A_{cts}/15{,}600)$ where A_{cts} is the area of concrete within the tensile zone at service loads after cracking (refer to DAfStB[31]). The parameter k_{f3} is a relaxation factor which has been introduced to the existing expression for k_{f2} in the revised version of AS3600-202X as a result of this study and is shown in Equation (6). This factor depends on the fiber type and duration of load. For short-term analyses, $k_{f3} = 1.0$ for all types of fibers. However, for determination of the final long-term crack widths after a period of sustained loading, it was demonstrated in the long-term tests by Watts et al.[32] and Watts et al.[33] that the tension provided by the fibers immediately after cracking (which leads to reductions in crack spacings) decays over time. Watts et al.[32] and Watts et al.[33] attributed this behavior to the gradual slip and/or deformability (i.e., creep and relaxation) of the fibers traversing a crack over time. Consequently, the stiffness of the cracked fiber reinforced section decreases over time. In members containing conventional reinforcement subjected to sustained loading, the loss of tension by the fibers is imparted to the conventional reinforcement. The reduction in tension provided by the synthetic fibers appears to be greater than for steel fibers due to the greater deformability (reduced modulus) of synthetic fibers. Additionally, the bond characteristics of both the steel and macro-synthetic fibers, defined by the physical shape of the fibers and their anchorage mechanisms, also contribute to the progressive slip of the fibers from the matrix over time, thus leading to a gradual degradation of the stiffness provided by the fibers across the crack. Similar conclusions were made by Boshoff and Nieuwoudt,[34] Babafemi et al.[35] and Vrijdaghs et al.[36] According to the testing undertaken by Watts et al.[32] and Watts et al.,[33] straight embossed polypropylene fibers appear to be less anchored and more susceptible to long-term debonding than end-hooked steel fibers. The relaxation factor k_{f3} has been calibrated to the results of the testing conducted by Watts et al.[32] and is taken as 0.3 for steel fibers and 0.1 for non-metallic fibers. For the case where fibers are not included (i.e., in plain reinforced concrete) $k_{f3} = 1$.

2.2 | Difference between reinforcement and concrete strains

The second term presented in Equation (1) represents the difference between the mean strain in the reinforcement and the mean strain in the concrete between the cracks. The mean strain in the concrete between the cracks includes the mean tensile stress-related strain and the shrinkage strain. The mean tensile stress-related strain is caused by the tensile stress that develops between the cracks due to the bond between the reinforcement and the surrounding concrete. This is made up of an elastic strain and a tensile creep strain. In AS3600, this difference is approximated by:

$$\varepsilon_{sm} - \varepsilon_{cm} = \frac{\sigma_{scr}}{E_s} - \frac{0.6 f_{ct}}{E_s \rho_{eff}}(1 + n_e \rho_{eff}) k_{f1} + \varepsilon_{cs}\left(1 - \frac{0.5 n_e \rho_{eff}}{1 + n_e \rho_{eff}}\right) \geq 0.6 \frac{\sigma_{scr}}{E_s}, \tag{7}$$

where ε_{cs} is the absolute value of the final long-term shrinkage strain, n_e is the effective modular ratio and is equal to $(1+\varphi_c)E_s/E_c$, φ_c is the creep coefficient

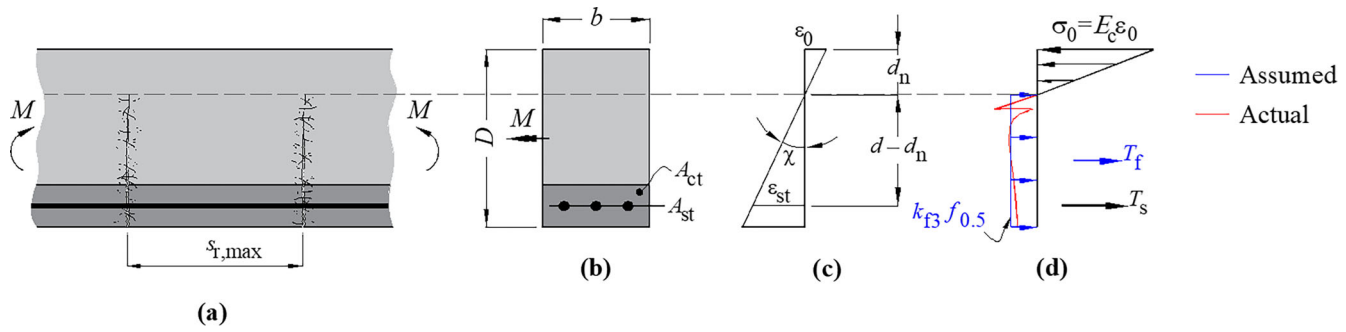

FIGURE 2 Serviceability limit state sectional analysis for fiber-reinforced concrete section in bending. (a) Beam elevation. (b) Section. (c) Strains at crack. (d) Stresses at crack.

associated with the time interval after cracking and E_s and E_c are the elastic moduli of the steel and concrete, respectively. The term k_{f1} accounts for the effect of the fibers (if any) on the tension stiffening effect. If no fibers are present, then $k_{f1} = 1.0$, otherwise if fibers are present

$$k_{f1} = 1 + \frac{k_{f3} f_{0.5}}{f_{ct}}. \tag{8}$$

In Equation (7), σ_{scr} is the stress in the tensile reinforcement assuming a cracked section at the time the crack width is required. It is important to note that a sectional analysis is required to evaluate this term whether or not fibers are contained in the section. Referring to the singularly reinforced FRC section in bending presented in Figure 2, a sectional analysis at the serviceability limit state for FRC assumes that the concrete is elastic in compression, the reinforcement is elastic in tension, and that the contribution of the fibers can be taken as rigid plastic applied to the tensile side of the neutral axis with a stress equal to $k_{f3}f_{0.5}$. Referring to Figure 2, σ_{scr} is evaluated as the strain in the longitudinal reinforcement, ε_{st}, multiplied by E_s. For a known moment, a sectional analysis may be completed by assuming a value of ε_{st} and solving for d_n:

$$d_n = \frac{-(A_{st}\varepsilon_{st}E_s + bk_{f3}f_{0.5}D + bk_{f3}f_{0.5}d) + \sqrt{(A_{st}\varepsilon_{st}E_s + bk_{f3}f_{0.5}D + bk_{f3}f_{0.5}d)^2 - 4(0.5bE_c\varepsilon_{st} - bk_{f3}f_{0.5})(-A_{st}\varepsilon_{st}E_s d - bk_{f3}f_{0.5}Dd)}}{2(0.5bE_c\varepsilon_{st} - bk_{f3}f_{0.5})}. \tag{9}$$

With all terms known in Equation (9), the strain at the extreme compressive fiber, ε_0, can be determined as $\varepsilon_{st} \times d_n/(d - d_n)$. The stress at the most extreme compressive fiber of the concrete is therefore $E_c\varepsilon_0$, and the resulting compressive force on the section is $0.5d_n bE_c\varepsilon_0$. The force carried by the fibers, T_f, is $k_{f3}f_{0.5}b(D - d_n)$ and the force in the steel reinforcement, T_s, is $\varepsilon_{st}E_sA_{st}$. The corresponding lever arms about the neutral axis for the compressive concrete, tensile fiber, and conventional steel reinforcement components are $2d_n/3$, $(D - d_n)/2$ and $d - d_n$, respectively. The solution procedure requires evaluation of the internal moment and, if required, ε_{st} is varied until the calculated internal moment is equal to the applied moment. The limiting term in Equation (7) is provided to limit the tension stiffening effects in members containing low reinforcement ratios.

Although the proposed method is based on the now-withdrawn 2004 edition of Eurocode 2 for reinforced concrete, which has recently been superseded by the 2024 version, the novelty of the approach is that the effect of the fibers may easily be incorporated into either model through the determination of the introduced factors k_{f1}, k_{f2}, k_{f3}, and k_g, which are applied to the expressions for crack spacing and the strain difference between the reinforcement and concrete. Should the next revision of AS3600 adopt the method proposed in the 2024 version of Eurocode 2 for plain reinforced concrete, the methodology proposed in this paper for FRC may still be extended without much effort.

3 | MODEL VALIDATION

The AS3600-2018 model for instantaneous loadings arrangements was previously validated by the authors in

Specimen ID	s_{r,max_exp} (mm)	s_{r,max_model} (mm)	$s_{r,max\_model}/s_{r,max\_exp}$
B-N-0.69	180.7	169.5	0.94
B-N-0.78	203.9	182.9	0.90
B-P-0.69	173.3	165.5	0.95
B-P-0.78	160.8	171.5	1.07
B-S-0.69	136.3	146.5	1.07
B-S-0.78	149.3	151.4	1.01

TABLE 1 Comparison of proposed model for maximum crack spacing to test data reported in Watts et al.[32]

Bernard et al.[37] This paper will therefore focus on validation for long term test data. In particular, the model is compared to the long-term test data reported in Watts et al.[32] To the authors' knowledge, this is the only comprehensive study available with full material characterization on large scale specimens subjected to a permanent service load. Watts et al.[32] subjected six large-scale specimens with varying fiber types (either no fibers, steel, or polypropylene fibers) of varying geometries and varying longitudinal reinforcement ratios to sustained uniformly distributed loads typically observed in practice. The specimens had the notation B-*X*-*Y* where "*X*" is the type of fiber (either "*S*" for steel, "*P*" for polypropylene or "*N*" for no fibers), and "*Y*" is the longitudinal tensile reinforcement ratio (in %). The dosage of the steel and polypropylene fibers adopted in that study was 30 and 5 kg/m^3, respectively.

With regard to crack spacing, Table 1 presents a comparison of the maximum crack spacing predicted using Equation (4) and that observed in the testing after approximately 600 days of testing.

Despite the considerable variation in predicted crack spacings, the proposed model adequately predicts the maximum crack spacing for each of the six specimens tested by Watts et al.,[32] with an average $s_{r,max\_model}/s_{r,max\_exp}$ of 0.99 and coefficient of variation equal to 7.3%. Certainly, more long-term test data is required for further validation; however, given the absence of a large database of test results, the model appears adequate in this respect.

Figure 3 presents a comparison of the maximum design crack widths evaluated according to the proposed model for each of the six specimens tested in Watts et al.[32] In Figure 3, the spread of widths for all cracks located within 400 mm of midspan is shown. It can be seen that the model typically falls well within the range of the recorded crack widths for all specimens over the entire duration of testing and predicts the average crack widths (i.e., the design crack widths) with good certainty. As such, the predicted crack widths are considered reasonable given the range and spread of the observed cracking. It is worth noting that the model tends to diverge somewhat at later ages for the polypropylene FRC relative to the steel FRC—this may be attributed to long-term effects such as shrinkage, creep, and relaxation of the fibers across the cracks. As noted earlier, further long-term testing is required by the scientific community to further validate the proposed model.

4 | EXAMPLE CALCULATIONS

To illustrate the ease of use of this model, this section provides example calculations for three reinforced concrete beams with the cross-section shown in Figure 2b. In these examples, $b = 300$ mm, $D = 500$ mm, $d = 450$ mm, $A_{st} = 930$ mm^2 (i.e., 3 × 20 mm diameter bars) and the clear cover to the longitudinal bars $c = 40$ mm. One beam contains steel fibers, one beam contains polypropylene fibers and the third beam contains no fibers. The beams are subjected to a maximum service load moment $M = 100$ kNm sustained over a long period of time. The material properties are $f'_c = 32$ MPa, $E_c = 28.6$ GPa, $f_{ct} = 2.5$ MPa, $\varepsilon_{cs} = 0.0006$, $\varphi_c = 2.5$, $E_s = 200$ GPa, and $f_{sy} = 500$ MPa. For both beams with fibers, $f_{0.5} = 1$ MPa.

4.1 | Case 1: steel fibers ($k_{f3} = 0.3$)

4.1.1 | Step 1

The first step involves determining the depth of the neutral axis d_n and therefore the strain profile. A reasonable first guess is to assume the stress in the bars is 200 MPa, giving $\varepsilon_{st} = 0.001$. d_n can be evaluated through Equation (9) as 128.29 mm. The strain in the extreme compressive fiber ε_0 is $0.001 \times 128.29/(450–128.29) = 0.000399$. The maximum compressive stress in the section is 11.40 MPa, giving a resulting compressive force, C equal to 219.45 kN. The force carried by the fibers is $0.3 \times 1 \times 300 \times (500–128.29) = 33.45$ kN and the force in the steel reinforcement is $0.001 \times 200{,}000 \times 930 = 186$ kN. The resulting internal moment can be evaluated as 84.83 kNm which is not equal to the applied moment of 100 kNm. Repeating this process with $\varepsilon_{st} = 0.001199$ (which can be obtained using goal seek) gives $d_n = 126.95$ mm, $\varepsilon_0 = 0.000471$, $\sigma_0 = 13.47$ MPa,

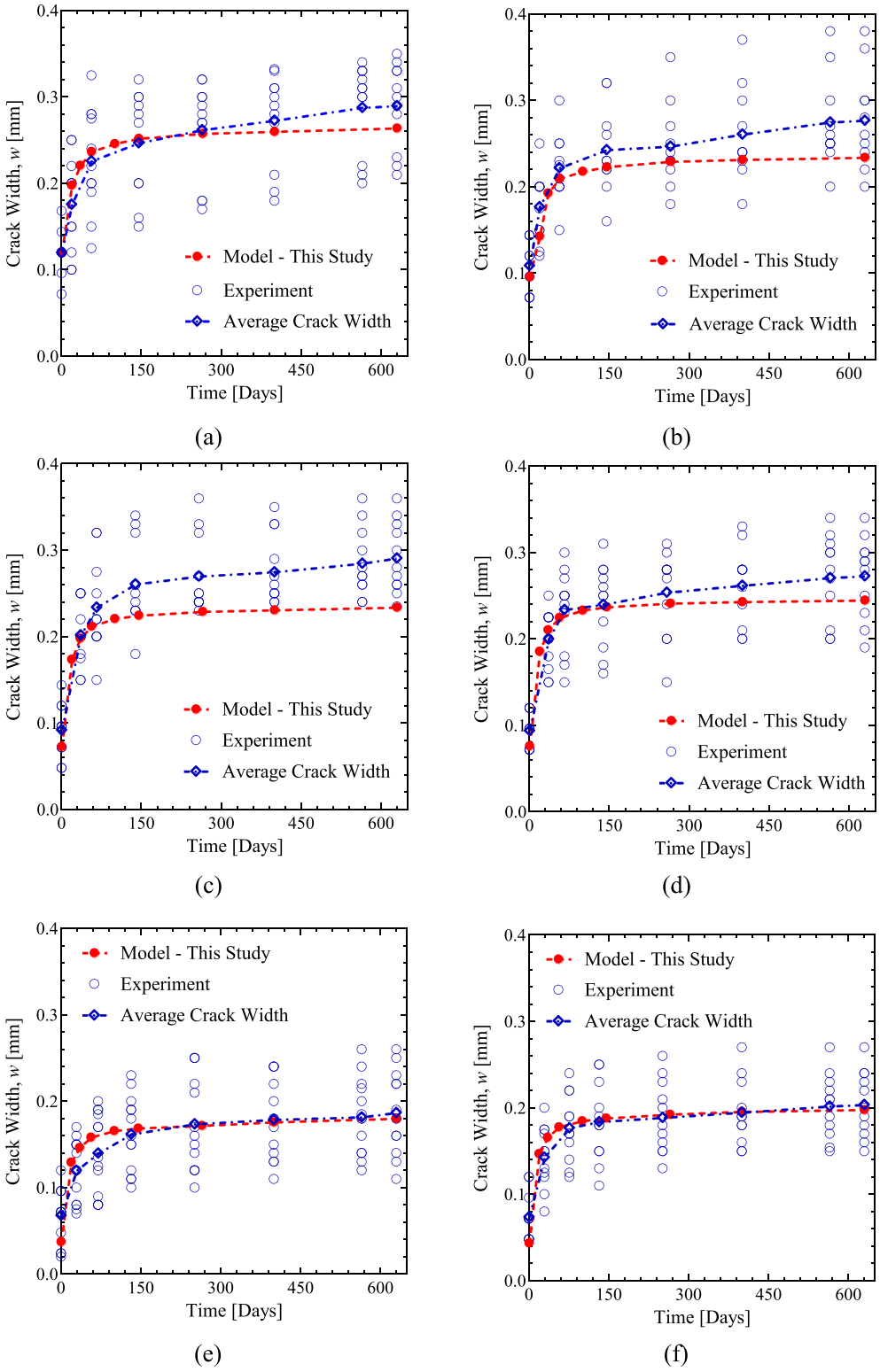

FIGURE 3 Comparison of proposed model to crack width data: (a) B-N-0.69; (b) B-N-0.78; (c) B-P-0.69; (d) B-P-0.78; (e) B-S-0.69; (f) B-S-0.78.

$C = 256.53$ kN, $T_f = 33.57$ kN, and $T_s = 222.96$ kN. In this case, the internal resisting moment is equal to 100 kNm which is equal to the applied moment. The concrete area within the tensile zone after cracking, $A_{cts} = b(D - d_n) = 111{,}916$ mm^2.

4.1.2 | Step 2

The member size factor at the serviceability limit state k_g and the modification factors to account for the effect of the fibers (k_{f1} and k_{f2}) are determined as follows

$$k_g = 1 + \left(\frac{0.0067 A_{cts}}{15{,}600}\right) = 1.048.$$

$$k_{f1} = 1 + \frac{k_{f3} f_{0.5}}{f_{ct}} = 1.12.$$

$$k_{f2} = \frac{\left(f_{ct} - 1.1\, k_g k_{f3} f_{0.5}\right)}{f_{ct}} = 0.862.$$

The effective modular ratio is $n_e = (1 + \varphi_c)\ E_s/E_c = 24.48$. The effective height $h_{c,eff} = (D - d_n)/3 = 124.35$ mm and the effective area of the tensile concrete is $A_{c,eff} = 300 \times 124.35 = 37{,}305\ mm^2$. The effective reinforcement ratio is $\rho_{eff} = A_{st}/A_{c,eff} = 0.0249$. The factors k_1 and k_2 in Equation (4) are 0.8 and 0.5, respectively.

4.1.3 | Step 3

The strain difference can be evaluated as

$$\begin{aligned}\varepsilon_{sm} - \varepsilon_{cm} &= \frac{239.74}{200{,}000} - \frac{0.6 \times 2.5}{200{,}000 \times 0.0249}(1 + 24.48 \times 0.0249)1.12 \\ &\quad + 0.0006\left(1 - \frac{0.5 \times 24.48 \times 0.0249}{1 + 24.48 \times 0.0249}\right) \\ &\geq 0.6\frac{237.74}{200{,}000} = 0.00114.\end{aligned}$$

The maximum crack spacing is evaluated following Equation (4):

$$\begin{aligned}s_{r,max} &= 0.86\left(3.4 \times 40 + \frac{0.3 \times 0.8 \times 0.5 \times 20}{0.0249}\right) \\ &\leq 1.3(500 - 126.95) = 200.1\ mm.\end{aligned}$$

4.1.4 | Step 4

The maximum crack width is evaluated following Equation (1):

$$w = s_{r,max}(\varepsilon_{sm} - \varepsilon_{cm}) = 200.1 \times 0.000114 = 0.229\ mm.$$

4.2 | Case 2: polypropylene fibers ($k_{f3} = 0.1$)

4.2.1 | Step 1

Repeating the process specified above, however, with $\varepsilon_{st} = 0.00127$ gives $d_n = 122.06$ mm, $\varepsilon_0 = 0.000474$, $\sigma_0 = 13.55$ MPa, $C = 248.16$ kN, $T_f = 11.34$ kN, and $T_s = 236.82$ kN. The internal resisting moment can be evaluated to equal 100 kNm, which is equivalent to the applied moment. The concrete area within the tensile zone after cracking, $A_{cts} = b(D - d_n) = 113{,}381\ mm^2$.

4.2.2 | Step 2

The member size factor at the serviceability limit state, k_g, and the modification factors to account for the effect of the fibers (k_{f1} and k_{f2}) are determined as follows.

$$k_g = 1 + \left(\frac{0.0067 A_{cts}}{15{,}600}\right) = 1.049.$$

$$k_{f1} = 1 + \frac{k_{f3} f_{0.5}}{f_{ct}} = 1.04.$$

$$k_{f2} = \frac{\left(f_{ct} - 1.1\, k_g k_{f3} f_{0.5}\right)}{f_{ct}} = 0.954.$$

The effective modular ratio is $n_e = (1 + \varphi_c)E_s/E_c = 24.48$. The effective height $h_{c,eff} = (D - d_n)/3 = 125.98$ mm and the effective area of the tensile concrete is $A_{c,eff} = 300 \times 125.98 = 37{,}794\ mm^2$. The effective reinforcement ratio is $\rho_{eff} = A_{st}/A_{c,eff} = 0.0246$. The factors k_1 and k_2 in Equation (4) are 0.8 and 0.5, respectively.

4.2.3 | Step 3

The strain difference can be evaluated as

$$\begin{aligned}\varepsilon_{sm} - \varepsilon_{cm} &= \frac{254.65}{200{,}000} - \frac{0.6 \times 2.5}{200{,}000 \times 0.0246}(1 + 24.48 \times 0.0246)1.04 \\ &\quad + 0.0006\left(1 - \frac{0.5 \times 24.48 \times 0.0246}{1 + 24.48 \times 0.0246}\right) \\ &\geq 0.6\frac{254.65}{200{,}000} = 0.00125.\end{aligned}$$

The maximum crack spacing is evaluated following Equation (4):

$$\begin{aligned}s_{r,max} &= 0.95\left(3.4 \times 40 + \frac{0.3 \times 0.8 \times 0.5 \times 20}{0.0246}\right) \\ &\leq 1.3(500 - 122.06) = 222.8\ mm.\end{aligned}$$

4.2.4 | Step 4

The maximum crack width is evaluated following Equation (1):

TABLE 2 Summary of example calculations.

Specimen	$(\varepsilon_{sm}-\varepsilon_{cm})$ (−)	$s_{r,max}$ (mm)	w (mm)
Case 1 (steel fibers)	0.00114	200.1	0.229
Case 2 (polypropylene fibers)	0.00125	222.8	0.279
Case 3 (no fibers)	0.00131	234.1	0.306

$$w = s_{r,max}(\varepsilon_{sm}-\varepsilon_{cm}) = 222.8 \times 0.000125 = 0.279\,\text{mm}.$$

4.3 | Case 3: no fibers ($f_{0.5} = 0$)

4.3.1 | Step 1

Repeating the process specified above, however, with $\varepsilon_{st} = 0.00131$ gives $d_n = 119.67$ mm, $\varepsilon_0 = 0.000475$, $\sigma_0 = 13.58$ MPa, $C = 243.84$ kN, $T_f = 0$ kN, and $T_s = 243.84$ kN. The internal resisting moment can be evaluated to equal 100 kNm, which is equivalent to the applied moment. The concrete area within the tensile zone after cracking, $A_{cts} = b(D - d_n) = 114{,}097$ mm^2.

4.3.2 | Step 2

The member size factor at the serviceability limit state k_g and the modification factors to account for the effect of the fibers (k_{f1} and k_{f2}) are determined as follows

$$k_g = 1 + \left(\frac{0.0067A_{cts}}{15{,}600}\right) = 1.049.$$

$$k_{f1} = 1 + \frac{k_{f3}f_{0.5}}{f_{ct}} = 1.$$

$$k_{f2} = \frac{\left(f_{ct} - 1.1\,k_g\,k_{f3}f_{0.5}\right)}{f_{ct}} = 1.$$

The effective modular ratio is $n_e = (1 + \varphi_c)E_s/E_c = 24.48$. The effective height $h_{c,eff} = (D - d_n)/3 = 126.78$ mm and the effective area of the tensile concrete is $A_{c,eff} = 300 \times 126.78 = 38{,}032$ mm^2. The effective reinforcement ratio is $\rho_{eff} = A_{st}/A_{c,eff} = 0.0244$. The factors k_1 and k_2 in Equation (4) are 0.8 and 0.5, respectively.

4.3.3 | Step 3

The strain difference can be evaluated as

$$\begin{aligned}\varepsilon_{sm}-\varepsilon_{cm} &= \frac{262.19}{200{,}000} - \frac{0.6 \times 2.5}{200{,}000 \times 0.0244}(1 + 24.48 \times 0.0244)1.0 \\ &\quad + 0.0006\left(1 - \frac{0.5 \times 24.48 \times 0.0244}{1 + 24.48 \times 0.0244}\right) \\ &\geq 0.6\frac{262.19}{200{,}000} = 0.00131.\end{aligned}$$

The maximum crack spacing is evaluated following Equation (4):

$$\begin{aligned}s_{r,max} &= 1.0\left(3.4 \times 40 + \frac{0.3 \times 0.8 \times 0.5 \times 20}{0.0244}\right) \\ &\leq 1.3(500 - 119.67) = 234.1\,\text{mm}.\end{aligned}$$

4.3.4 | Step 4

The maximum crack width is evaluated following Equation (1):

$$w = s_{r,max}(\varepsilon_{sm}-\varepsilon_{cm}) = 234.1 \times 0.000131 = 0.306\,\text{mm}.$$

Table 2 presents a summary of the results of the preceding analyses. It can be seen that the addition of a moderate amount of steel fibers results in an approximately 25% and 15% reduction in the design crack width and maximum crack spacing, respectively, relative to the case where no fibers are present. On the other hand, the polypropylene mix with equivalent $f_{0.5}$ results in only a 9% and 5% reduction in the design crack width and maximum crack spacing, respectively, relative to the case where no fibers are present. This is a result of the adopted k_{f3} values for each fiber type.

5 | CONCLUDING REMARKS

This paper provides background for the expressions given in the updated Australian Concrete Structures Standard (AS3600-202X) with respect to flexural crack widths in FRC elements containing conventional reinforcement. The proposed model has been adapted from the existing expression for plain reinforced concrete and accounts for the beneficial effects of the fibers (steel and polypropylene) in the short- and long-term. The benefit of this approach is

that a single expression may be used to determine the short- and long-term cracking behavior of reinforced or FRC elements subjected to flexure. The model is validated against the long-term test data provided in Watts et al.[32] Sample calculations are provided to illustrate the ease-of-use of the model.

ACKNOWLEDGMENTS

This work was supported by an Australian Research Council Discovery Grant (DP 200102114) awarded to the first and second authors as well as an Australian Research Council Industry Fellowship awarded to the first author (IE240100025). Open access publishing facilitated by The University of Sydney, as part of the Wiley - The University of Sydney agreement via the Council of Australian University Librarians.

CONFLICT OF INTEREST STATEMENT

None of the authors have a conflict of interest to disclose.

DATA AVAILABILITY STATEMENT

Data sharing not applicable to this article as no datasets were generated or analysed during the current study.

ORCID

Ali Amin https://orcid.org/0000-0002-9088-8634
E. Stefan Bernard https://orcid.org/0000-0002-3445-5308

REFERENCES

1. Tiberti G, Trabucchi I, AlHamaydeh M, Minelli F, Plizzari GA. Crack development in steel fibre reinforced concrete members with conventional rebars. Mag Concr Res. 2018;71:599–610. https://doi.org/10.1680/jmacr.17.00361
2. Chiaia B, Fantilli AP, Vallini P. Evaluation of crack width in FRC structures and application to tunnel linings. Mater Struct. 2009;42:339–51. https://doi.org/10.1617/s11527-008-9385-7
3. Watts MJ, Amin A, Gilbert RI, Kaufmann W, Minelli F. Simplified time-dependent crack width prediction for fiber reinforced concrete flexural members. Struct Concr. 2021;22(3):1549–60. https://doi.org/10.1002/suco.202000683
4. Amin A, Gilbert RI. Instantaneous crack width calculation for steel fiber-reinforced concrete flexural members. ACI Struct J. 2018;115:535–43. https://doi.org/10.14359/51701116
5. Amin A, Foster SJ. Shear strength of steel fibre reinforced concrete beams with stirrups. Eng Struct. 2016;111:323–32. https://doi.org/10.1016/j.engstruct.2015.12.026
6. Minelli F. Plain and fiber reinforced concrete beams under shear loading: structural behavior and design aspects. PhD dissertation. Brescia: Department of Civil Engineering, University of Brescia. 2005.
7. Deluce JR, Vecchio FJ. Cracking behavior of steel fiber reinforced concrete members containing conventional reinforcement. ACI Struct J. 2013;110(3):481–90.
8. Pfyl T. Tragverhalten von Stahlfaserbeton. PhD dissertation, IBK-Report No. 279. Swiss Federal Institute of Technology (in German). 2003.
9. Amin A, Foster SJ, Watts M. Modelling the tension stiffening effect in SFR-RC. Mag Concr Res. 2016;68(7):339–52. https://doi.org/10.1680/macr.15.00188
10. Marti P, Alvarez M, Kaufmann W, Sigrist V. Tension chord model for structural concrete. Struct Eng Int. 1998;8(4):287–98. https://doi.org/10.2749/101686698780488875
11. Amin A, Foster SJ, Kaufmann W. Instantaneous deflection calculation for steel fiber reinforced concrete one-way members. Eng Struct. 2017;131:438–45. https://doi.org/10.1016/j.engstruct.2016.10.041
12. Markic T, Amin A, Kaufmann W, Pfyl T. Strength and deformation capacity of tension and flexural RC members containing steel fibers. J Struct Eng. 2020;146(5):04020069. https://doi.org/10.1061/(ASCE)ST.1943-541X.0002614
13. AS3600. Australian Standard, concrete structures. Sydney: Standards Australia; 2018.
14. fib. *fib* Model Code 2010. Lausanne: Fédération Internationale du Béton; 2013.
15. fib. *fib* Model Code 2020. Lausanne: Fédération Internationale du Béton; 2023.
16. EN 1992-1-1. Eurocode 2. Design of concrete structures. General rules for buildings. 2004.
17. EN 1992-1-1. Eurocode 2. Design of concrete structures. General rules for buildings, bridges and civil engineering structures. 2024.
18. Balazs GL, Bisch P, Borosnyoi A, Burdet O, Burns C, Ceroni F, et al. Design for SLS according to *fib* Model Code 2010. Struct Concr. 2012;14(2):99–123. https://doi.org/10.1002/suco.201200060
19. Debernardi PG, Taliano M. An improvement to Eurocode 2 and *fib* Model Code 2010 methods for calculating crack width in RC structures. Struct Concr. 2015;17(3):365–76. https://doi.org/10.1002/suco.201500033
20. van der Esch A, Wolfs R, Fennis S, Roosen M, Wijte S. Categorization of formulas for calculation of crack width and spacing in reinforced concrete elements. Struct Concr. 2024;25:32–48. https://doi.org/10.1002/suco.202300535
21. Terjesen O, Pinto G, Kanstad T, Tan R. Performance study of crack width calculation methods according to Eurocodes, *fib* model codes and the modified tension chord model. Struct Concr. 2024;25:2375–99. https://doi.org/10.1002/suco.202300367
22. Cervenka V, Rimkus A, Gribniak V, Cervenka J. Simulation of the crack width in reinforced concrete beams based on concrete fracture. Theor Appl Fract Mech. 2022;121:103428. https://doi.org/10.1016/j.tafmec.2022.103428
23. Gilbert RI, Ranzi G. Time-dependent behaviour of concrete structures. London: CRC Press; 2011.
24. Schlicke D, Dorfmann EM, Fehling E, Viet Tue N. Calculation of maximum crack width for practical design of reinforced concrete. Civ Eng Des. 2021;3:45–61.

25. Borosnyoi A, Balazs GL. Models for flexural cracking in concrete: the state of the art. Struct Concr. 2005;6(2):53–62. https://doi.org/10.1680/stco.2005.6.2.53
26. Kaufmann W, Mata-Falcon J, Amin A. Compression field analysis of fiber-reinforced concrete based on the cracked membrane model. ACI Struct J. 2019;116(5):213–24.
27. Beeby AW. The influence of the parameter φ/ρeff on crack widths. Struct Concr. 2005;6:155–65. https://doi.org/10.1680/stco.2005.6.4.155
28. Ferry-Borges J. Cracking and deformability of reinforced concrete beams. Association International des Ponts et Charpentes. 1966.
29. Caldentey AP, Garcia R, Gribniak V, Rimkus A. Tension versus flexure: Reasons to modify the formulation of MC 2010 for cracking. Struct Concr. 2020;21:2101–23. https://doi.org/10.1002/suco.202000279
30. Tang P, Amin A, Gilbert RI, Kaufmann W. Shrinkage cracking in restrained FRC members containing conventional reinforcement. Struct Concr. 2024;25(2):1006–17.
31. DAfStB. Richtlinie Stahlfaserbeton. Berlin: Deutscher Ausschuss fur Stahlbeton (in German). 2012.
32. Watts M, Amin A, Gilbert RI. Time-dependent deformation and cracking behaviour of FRC beams. Eng Struct. 2022;268:114741.
33. Watts M, Amin A, Gilbert RI. Time-dependent elongation and cracking behavior of fiber reinforced concrete tension chords. Struct Concr. 2023;24(1):1436–51.
34. Boshoff WP, Nieuwoudt PD. Tensile creep of cracked steel fibre reinforced concrete: mechanisms on the single fibre and at the macro level. In: Serna P, Llano-Torre A, Cavalaro SHP, editors. Proceedings of the International RILEM Workshop FRC-Creep 2016. Dordrecht: Springer; 2017. p. 63–75.
35. Babafemi AJ, du Plessis A, Boshoff WP. Pull-out creep mechanism of synthetic macro fibres under a sustained load. Construct Build Mater. 2018;174:466–73.
36. Vrijdaghs R, di Prisco M, Vandewalle L. Uniaxial tensile creep of a cracked polypropylene fiber reinforced concrete. Mater Struct. 2018;51:5.
37. Bernard ES, Amin A, Gilbert RI. Assessment of MC2010 and AS3600 models for estimating instantaneous flexural crack widths in fibre reinforced concrete members. Eng Struct. 2020;208:110271.

AUTHOR BIOGRAPHIES

Ali Amin, School of Civil Engineering, The University of Sydney, Sydney, New South Wales, Australia. Email: ali.amin@sydney.edu.au.

R. Ian Gilbert, School of Civil and Environmental Engineering, The University of New South Wales, Sydney, New South Wales, Australia. Email: i.gilbert@unsw.edu.au.

E. Stefan Bernard, Institute for Sustainable Industries and Liveable Cities (ISILC), Victoria University, Melbourne, Victoria, Australia. Email: s.bernard@tse.net.au.

How to cite this article: Amin A, Gilbert RI, Bernard ES. Flexural crack control in fiber-reinforced concrete according to AS3600. Structural Concrete. 2025. https://doi.org/10.1002/suco.70255